Wind Tunnel Experiment of Wind-Induced Single-sided Ventilation under Generic Sheltered Urban Area

Zitao Jiang*[1], Tomohiro Kobayashi[1], Toshio Yamanaka[1], Noriaki Kobayashi[1], Narae Choi[3], Mats Sandberg[2], Kayuki Sano[1], and Kota Toyosawa[1]

1 Osaka University
2-1 Yamadaoka
Suita City, Japan
**Corresponding author:*
jiang_zitao@arch.eng.osaka-u.ac.jp

2 University of Gävle
SE-801 7
Gävle, Sweden

3 Toyo University
5 Chome-28-20 Hakusan
Tokyo, Japan

ABSTRACT

The utilization of natural ventilation helps to reduce building energy consumption and improve indoor air quality. In the urban area, the performance of the natural ventilation is very sensitive to surrounding building density. However, the influence of surrounding buildings on ventilation rate was not well investigated in previous research. This paper presents a wind tunnel experiment to assess the influence of urban density on the wind-induced ventilation rate of single-sided ventilation. Spacing density, wind direction, and the number of openings were primary factors that were investigated in this experiment. The ventilation rate is evaluated by a continuous dose method of the tracer gas technique. The wind pressure coefficient at openings of the sealed model without openings was measured by pressure transduces. The streamwise velocity at the street canyon was measured by a split-film probe with a constant temperature anemometer unit. The ventilation rate, wind pressure coefficient fluctuations, and surrounding velocity of an isolated building are compared to that of a building with two layers of surrounding buildings with a spacing of 0.5 H (building height), 1 H, and 1.5 H. The relationship between the wind pressure coefficient of the sealed model and the ventilation rate was also discussed.

KEYWORDS

Natural ventilation, Wind pressure coefficients; Wind tunnel experiment, Urban canopy flow

1 INTRODUCTION

Accurately predicting natural ventilation rates and understanding its performance in different environmental conditions is crucial for optimizing building ventilation design. However, predicting natural ventilation rates can be challenging due to the complex interactions between wind flow, building geometry, and other factors. Moreover, the effectiveness of natural ventilation systems can be significantly affected by external factors such as wind direction and building orientation (Y. Jiang & Chen, 2002), especially in sheltered conditions (Ghiaus et al., 2006) where airflow is limited. The sheltering effect on cross ventilation was extensively investigated by wind tunnel experiments or numerical analysis (Tominaga & Blocken, 2015; Ikegaya et al., 2019; Shirzadi et al., 2019; Adachi et al., 2020; Golubić et al., 2020; Mohammad et al., 2021). In the urban context, compared to cross ventilation, single-sided ventilation is a more common ventilation feature because of the limitation of large indoor spaces. Focusing on single-sided ventilation in isolated and sheltered buildings, this research has two-fold purposes. The first objective is to investigate the sheltering effect of single-sided ventilation. The second aim of the present work is to look into the wind pressure fluctuation that is dominating wind-induced ventilation and discuss the ventilation rate prediction methods of single-sided ventilation.

2 EXPERIMENT METHODS

2.1 Case and wind tunnel descriptions

The target building model is a cube with the dimension of 100 mm (Length) x 100 mm (Width) x 100 mm (Height). Two types of building models were used: one is the sealed model without openings, which was used to measure the wind pressure coefficient, and the other is the building model with openings, which was used to evaluate the ventilation performance. For the building model with openings, as shown in Fig.1(a), it is assumed the target building model has 1/2/3 square-shaped openings (15mm x 15mm) located on the same external wall, which are abbreviated as SS1, SS2 and SS3.

Both isolated and sheltering conditions were tested in the experiment. The surrounding buildings have the same dimension as the target cubical building but without openings, and two layers of surroundings were arranged in a regular array with equal spacing of d, which is d=0.5H, d=1H and d=1.5H respectively. The planar area ratio (λ_p) is defined as:

$$\lambda_p = \frac{LW}{(L+d)(W+d)} \tag{1.}$$

where L and W are the length and width of the target building, and d is the distance between adjacent buildings. λ_p is λ_p =0.44, λ_p =0.25 and λ_p =0.16 in three sheltering cases respectively.

The approaching wind direction is set to 0°(opening at windward side), 30°, 45°, 60°, 90°(opening at lateral side), 120°, 135°, 150° and 180°(opening at leeward side). The turntable was rotated to accommodate the different approaching wind directions. The combination of opening configuration, sheltering condition and approaching wind angle resulted in a total of 108 cases in this experiment.

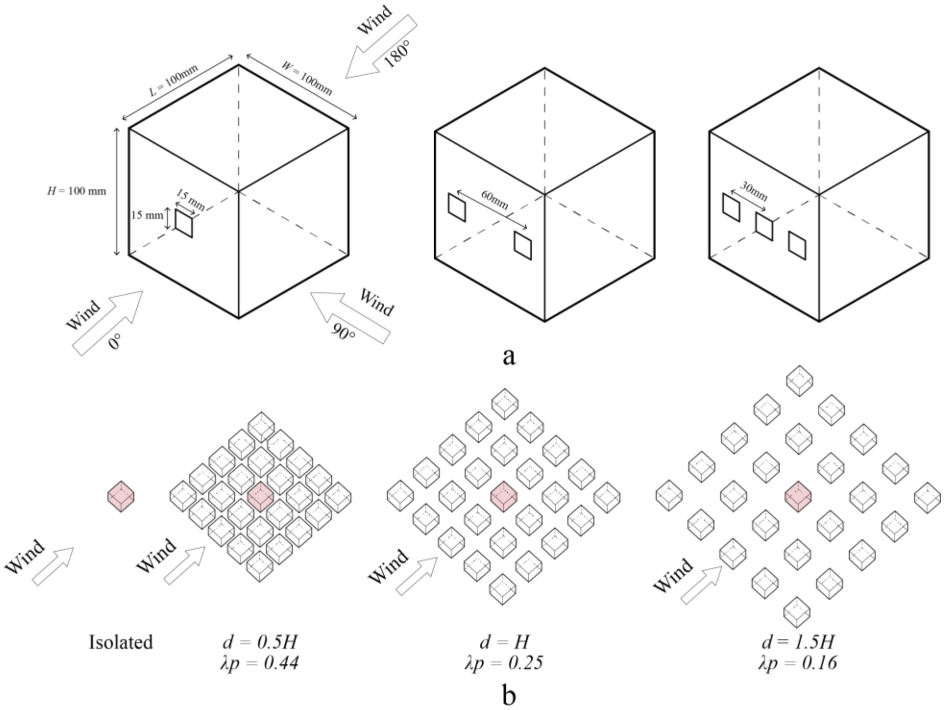

Fig. 1. (a) Schematic view of the studied cubic building model; (b) Surrounding building configurations.

The wind tunnel experiment was carried out in the atmospheric boundary layer wind tunnel at Osaka University. A combination of turbulence grid and roughness blocks were used to create a neutral atmospheric boundary layer as shown in Fig.2(a). Fig.2(b) shows the experimental setup for the ventilation performance measurement. The vertical mean streamwise velocity profiles and turbulent intensity measured at the centre of the turntable without the physical models are shown in Fig.2(c) and Fig.2(d). The reference velocity at building height (U_H) was measured to be 6.44 m/s.

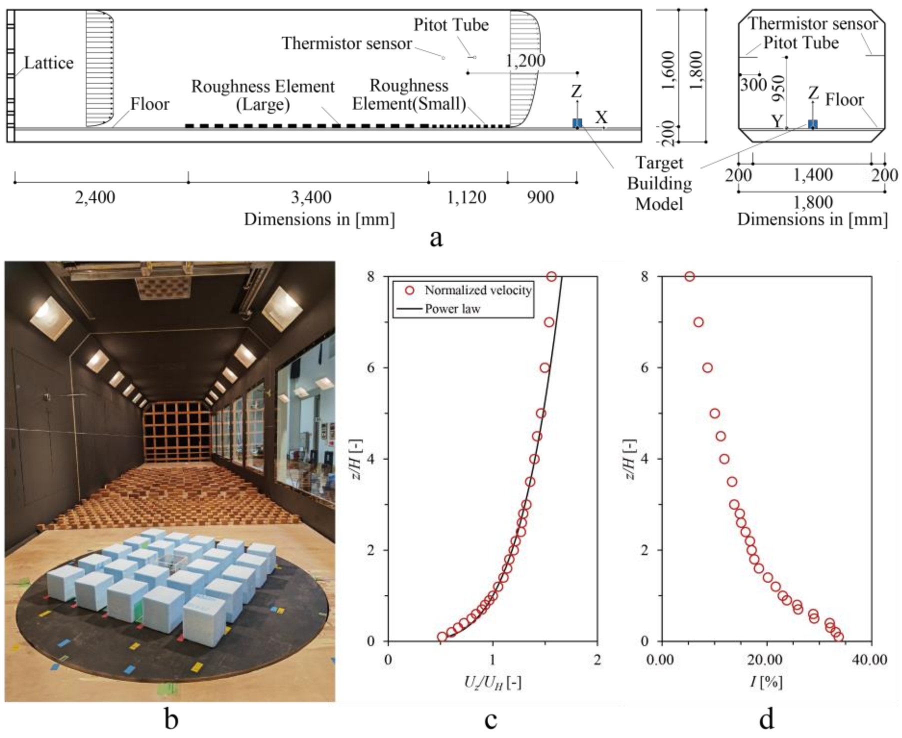

Fig. 2. (a) Wind tunnel schematic diagram; (b) Inside view of the wind tunnel; (c) Mean streamwise velocity of the boundary layer; (d) Turbulence intensity of the boundary layer.

2.2 Velocity measurement

The streamwise velocity component of flow (U_x) in the street canyon were measured by the straight split-fibre film probe (55R55, Dantec) in the wind tunnel experiment. The probe was operated using a constant-temperature anemometer and linearizer modules (Kanomax). Sampling was conducted at a rate of 1,000 Hz for a period of 60 s for the velocity measurements to obtain statistically stationary values.

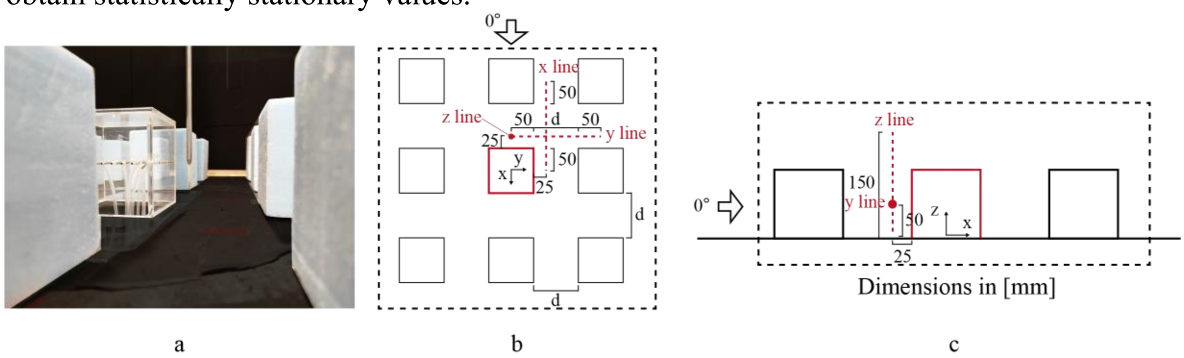

Fig. 3. (a) Photo of velocity measurement by split-fibre film probe; (b) Plan view of measurement lines; (c) Section view of measurement lines.

Fig.3(a) shows the velocity measurement set-up in the wind tunnel. The nearby velocity around the sealed model with 0° wind direction under different planar density cases was measured. Fig.3(b) and Fig.3(c) show three velocity measurement lines around the building. In each condition, wind speeds are measured at a 25 mm distance from the building wall in three lines in the X-, Y- and Z-directions at 10 mm intervals. Measurement lines X and Y are 50 mm above the wind tunnel ground.

2.3 Pressure coefficient measurement

The mean and fluctuating pressure at the three opening positions at the sealed building model were measured as shown in Fig.4(a) and Fig.4(b). Wind pressure is commonly expressed by wind pressure coefficient (Cp), which is defined as the ratio of wind pressure at the point of the sealed body and the reference dynamic pressure in free-stream flow.

$$Cp = \frac{p - p_{ref}}{p_d} \tag{2.}$$

where p is the static pressure at the wall of the sealed model, p_{ref} is the reference static pressure in approaching flow and p_d is the dynamic pressure at building height (100 mm). Both mean and RMS of Cp are measured by connecting surface pressure taps and a pressure transducer (Validyne DP45). The pressure was measured at a frequency of 1000 Hz for 60 s in the experiment to obtain high-frequency data.

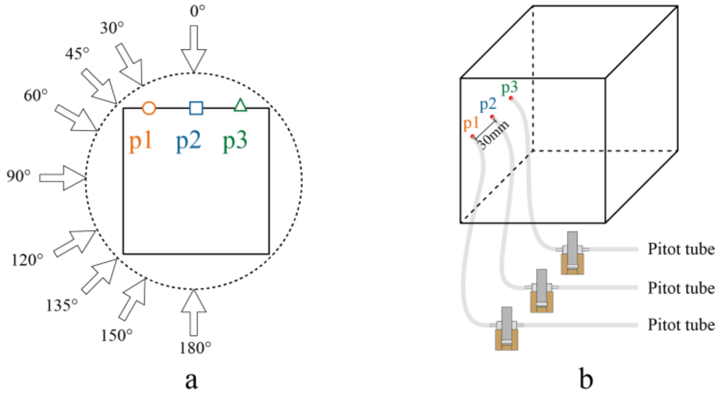

Fig. 4. (a) Wind pressure measurement points; (b) Pressure measurement system.

2.4 Ventilation rate measurement

In this study, the ventilation rate was evaluated by the continuous dose method of the tracer gas technique. CO_2 was used as the tracer gas in the experiment. Fig.5 shows the diagram of the ventilation rate measurement system. The tracer gas was evenly injected from 4 evenly distributed dosing pipes, the emission rate was controlled by a mass flow controller (Fujikin, FCS-T1005F). The tracer gas concentration at the centre of the physical building model was sampled by a sampling pipe, and concentration was measured by a gas analyser (LumaSence Technologies, Innova 1312).

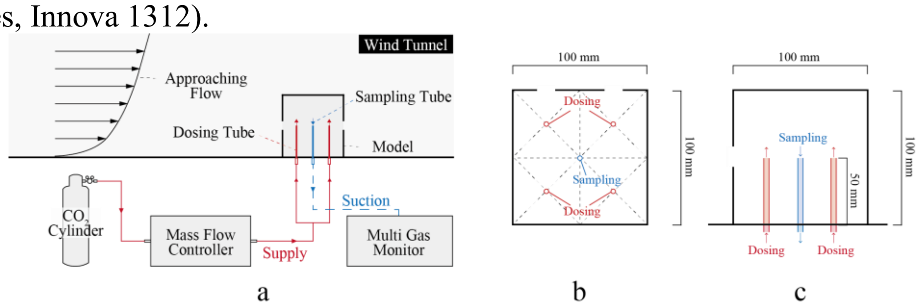

Fig. 5. (a) Schematic of the tracer gas measurement; (b) Plan view of tracer gas injection and sampling rods; (c) Section view of tracer gas injection and sampling rods

The wind tunnel was switched to open-circuit to prevent the influence of returning tracer gas from upstream. The measurement procedure involved first recording the indoor concentration without CO_2 emission for 5 minutes, during which the average value was taken as the mean outdoor concentration. Subsequently, measurements were carried out every 1 minute for 10 minutes after the indoor concentration reached a steady state.

$$Q = \frac{m}{C_r - C_o} \tag{3.}$$

where m is the constant volumetric emission rate of tracer gas $[m^3/s]$, C_r and C_o are time-averaged steady-state indoor and outdoor concentrations respectively. In this study, the dimensionless ventilation rate Q' is defined ($Q' = Q/\ AU_H$) as the measured ventilation rate (Q, m^3/s) divided by the product of a single opening area (A=*2.25*$\times 10^{-4} m^2$) and building height velocity ($U_H = 6.44\ m/s$).

3 RESULTS

3.1 Velocity results

Fig.6 shows the velocity measurement results, the positive velocity is the streamwise direction and the negative velocity is the reverse flow. Fig.6(a) shows the mean streamwise velocity along the X-direction measurement line. For isolated building, the obstruction of the windward wall makes the flow velocity experiences a gradual increase when approaching the building, and the velocity reaches the peak value (U_x/U_H=0.94) at a short distance downstream of the corner (x/H=-0.4). Fig.6(b) shows the mean streamwise velocity along the Y-direction measurement line. In all conditions, the velocity increases from the centre of the windward side (y/H=0) to the street ventilation corridor, and it reaches the peak at the centre of the ventilation corridor. It can be observed that the velocity in sheltering cases is negative outside of the ventilation corridor, which is caused by the recirculating flow in the wake region of the upwind building. Fig.6(c) shows the mean streamwise velocity along the Z-direction measurement line. For isolated buildings, the reverse flow only occurs at the lowest part of the measurement line. In sheltering cases, the reverse flows are observed from the ground up to the height of the building (z/H=0.9). Similar to velocity results along the Y measurement line, it is thought to be due to the effect of the circulation flow caused by the building on the windward side. Moreover, the higher position of reverse flow also indicates the centre of the eddy vortex in the street canyon moves higher.

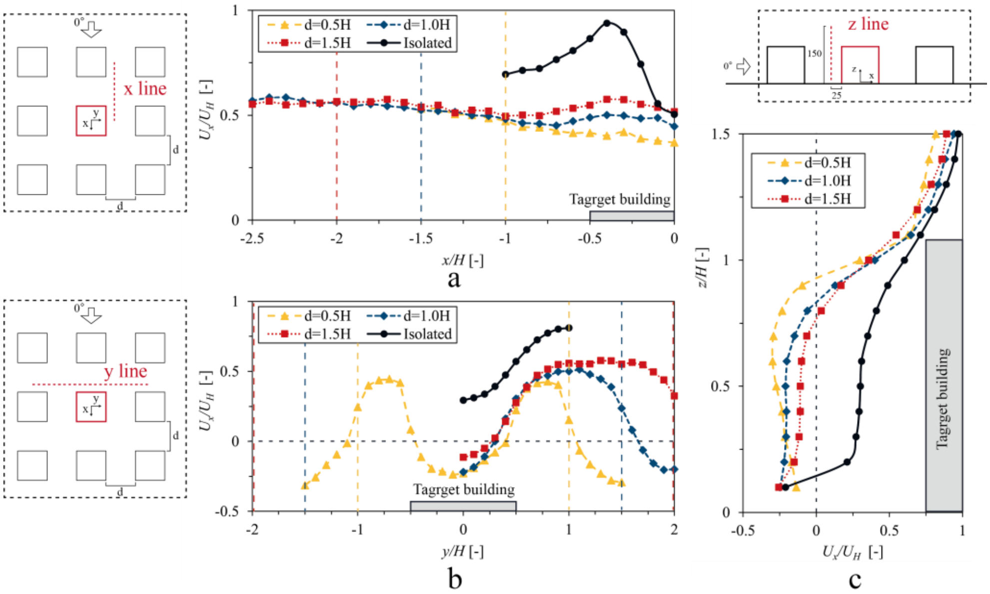

Fig. 6. (a) Mean streamwise velocity at X direction measurement line; (b) Mean streamwise velocity at Y direction measurement line; (c) Mean streamwise velocity at Z direction measurement line.

3.2 Wind pressure coefficient results

Fig.7 plots the time-averaged Cp ($\overline{Cp}$) and RMS of Cp (σ_{Cp}) at three measurement points against different wind directions under different conditions. The results show that for isolated cases, the value of $\overline{Cp}$ changes significantly as the wind direction changes. $\overline{Cp}$ decreases when the wind direction increases between 0° and 90°, and $\overline{Cp}$ increases between the wind direction of 120° and 180°. In the condition where there are surrounding buildings, the change becomes smaller as the building spacing becomes narrower and the $\overline{Cp}$ value also becomes smaller.

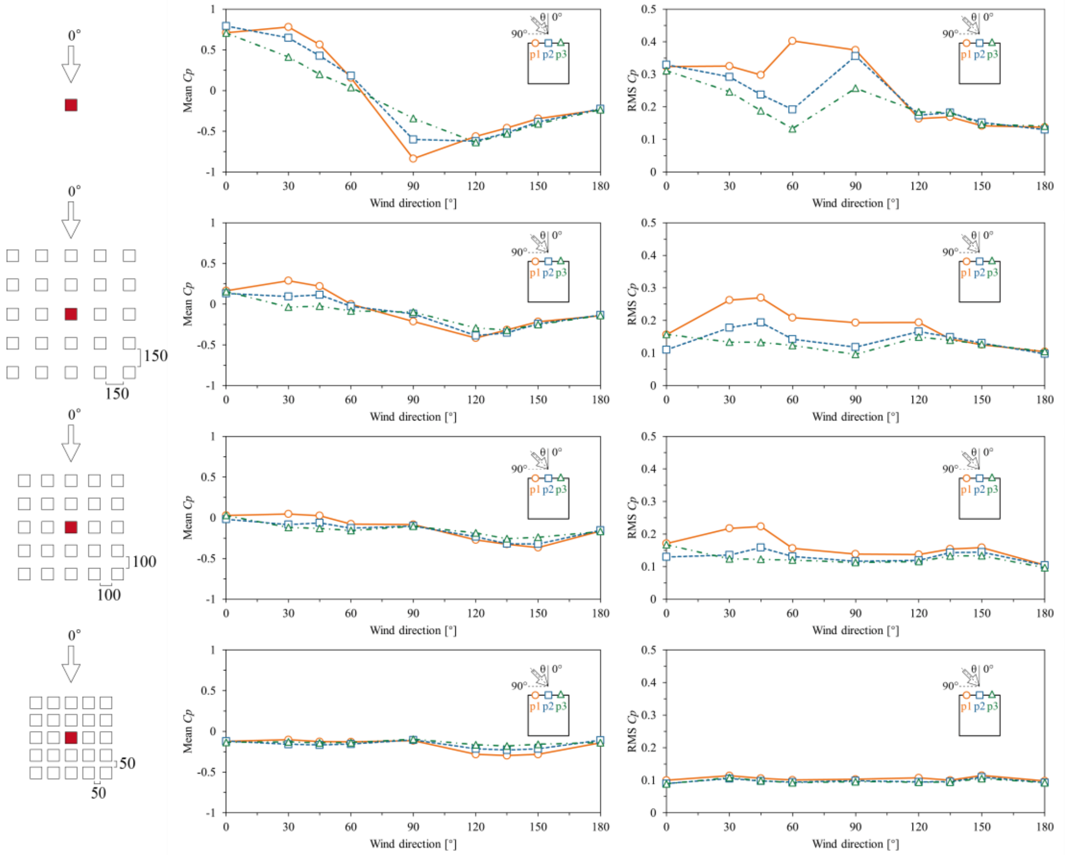

Fig. 7. Mean Cp of three measurement points against different wind angles under different sheltering conditions.

Considering the SS2 case, ventilation is predominantly determined by the pressure difference between point 1 and point 3. The mean wind pressure difference ($\overline{\Delta Cp}$) and RMS of the wind pressure difference between point 1 and point 3 is shown in Fig.8. Generally, compared to isolated cases, $\overline{\Delta Cp}$ becomes smaller when there are surrounding buildings.

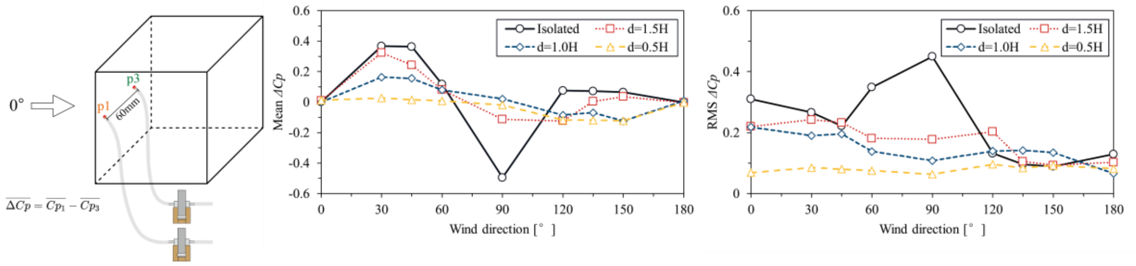

Fig. 8. Mean ΔCp against different wind angles under different sheltering conditions.

3.3 Ventilation rate results

Fig.9 (a) shows the *Q'* against different wind directions classified by the number of openings. In SS1 case, *Q'* tends to be slightly higher when the opening faces upwind. In a higher density case (Case 0.5H), since the airflow in the street canyon and wind pressure fluctuations are more invariant to wind directions, the *Q'* are nearly unchanged wherever the approaching wind comes. The trend of *Q'* in SS2 cases and SS3 cases are rather similar, *Q'* is very sensitive to both sheltering conditions and wind directions. When the wind direction is between 0° and 60°, or at around 90, *Q'* is relatively higher than others in wind directions. Fig.9(b) shows the *Q'* against different wind directions classified by the spacing between buildings. *Q'* of SS2 and SS3 cases are much higher than that of SS1 cases. The difference in *Q'* between SS2 and SS3 cases is insignificant.

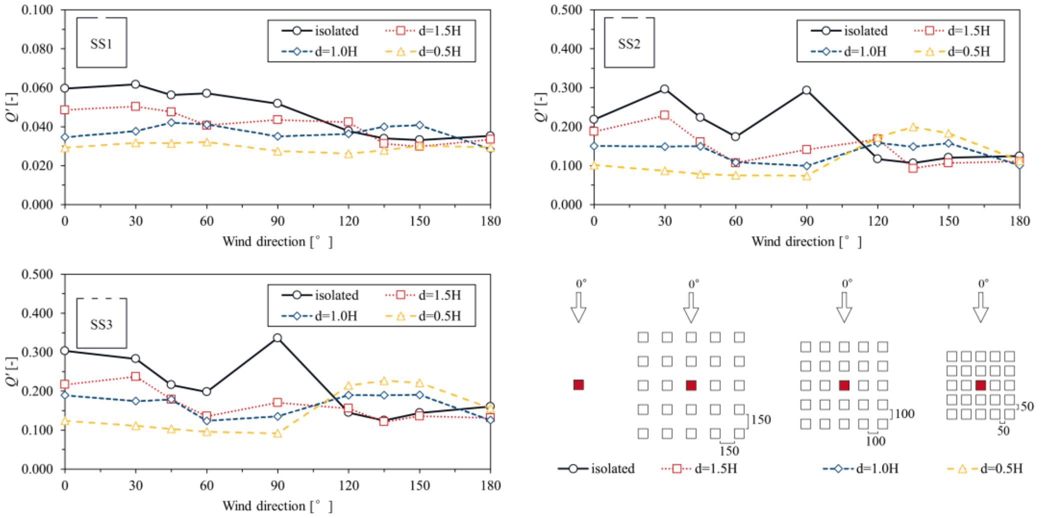

a

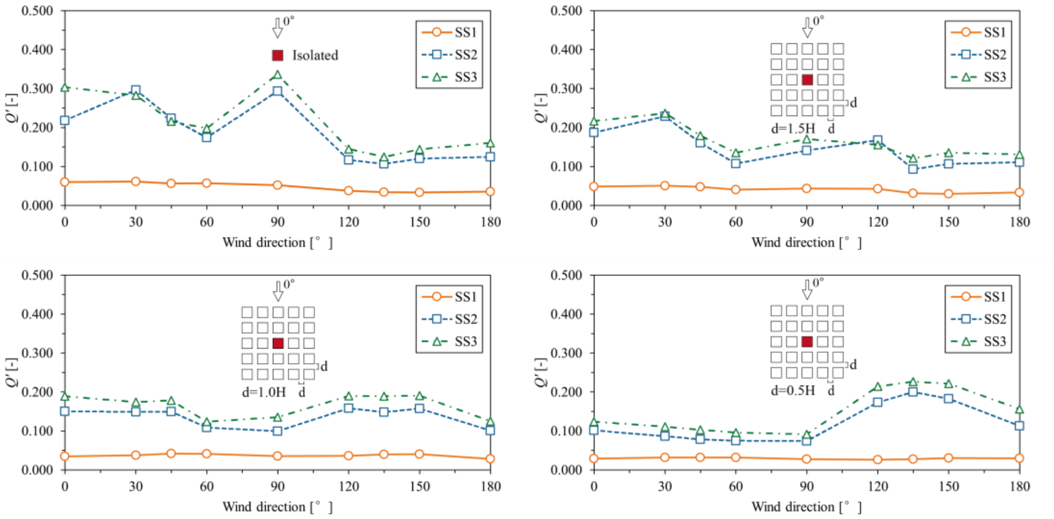

b

Fig. 9. (a) Dimensionless ventilation rate (Q') against different wind directions for SS1/SS2/SS3 cases; (b) Dimensionless ventilation rate (Q') against different wind directions for isolated/d=1.5H/d=1.0H/d=0.5H cases

3.4 Relation between SS1 ventilation rate and pressure

In SS1, it is assumed that time-averaged pressure between indoor and outdoor is almost the same, therefore, the pressure fluctuations at the openings mainly contribute to air exchange between indoor and outdoor air. Fig.10(a) shows the relations between $\sqrt{\sigma_{Cp}}$ and dimensionless measured ventilation rate Q' for SS1 cases. The Pearson correlation between $\sqrt{\sigma_{Cp}}$ and Q' was found to be 0.80, which indicates there is a relatively positive linear correlation between the pressure fluctuations and the ventilation rate. The constant C was determined by the least square method, resulting in a value of 0.1022. Using σ_{Cp}, the ventilation rate can be simply estimated by Eq.(4).

$$Q = CAU_{ref}\sqrt{\sigma_{Cp}} \tag{4.}$$

Fig.10(b) plots the measured ventilation rate and predicted ventilation rate from Eq.(4). The absolute error in the prediction is defined as:

$$\frac{1}{n}\sum_{i=1}^{n}\left|\frac{Q'_{pre} - Q'}{Q'} \cdot 100\%\right| \tag{5.}$$

The dotted line in Fig.10(b) represents the 30% deviation from the *y*=*x* line. Analysis of the data reveals that the majority of predicted ventilation rates exhibit an absolute error of less than 30%. Furthermore, the proposed prediction equation has an absolute error of 11% when applied to all measured values, indicating good accuracy.

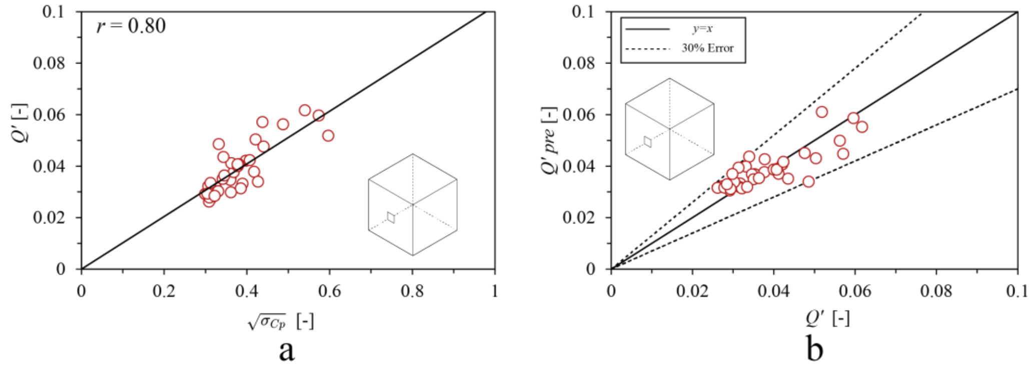

Fig. 10. SS1 ventilation prediction methods (a) Relations between $\sqrt{\sigma_p}$ and dimensionless ventilation rate Q'; (b) Comparison between measured ventilation rate Q' and predicted ventilation rate Q'_{pre}

3.5 Relation between SS2 ventilation rate and pressure

As pointed out by much previous research, not only mean pressure difference but also pressure difference pressure contributes to part of the ventilation rate (Chu et al., 2015; Daish et al., 2016; Z. Jiang et al., 2022). Fig.11(a) shows the relations between $\sqrt{\sigma_{\Delta Cp}}$ and dimensionless measured ventilation rate Q' for SS2 cases. The Pearson correlation between $\sqrt{\sigma_{\Delta Cp}}$ and Q' was found to be 0.76, which indicates there is a relatively positive linear correlation between the pressure difference fluctuations and the ventilation rate.

In previous research, it was widely accepted that the Orifice equation fails to well predict the wind-induced ventilation rate when the $\overline{\Delta Cp}$ is small. It is the consequence of bi-directional airflow that makes the inlet and outlet alternatively change between two openings and the predicted ventilation rate based on $\overline{\Delta Cp}$ will underestimate the ventilation performance. In this study, instead of using the absolute value of the mean wind pressure coefficient ($|\overline{\Delta Cp}|$), the time average of the absolute wind pressure coefficient ($\overline{|\Delta Cp|}$) was used to predict the ventilation rate.

$$\mathrm{Q} = (C_d A)_{eff} U_{ref}\sqrt{\overline{|\Delta Cp|}} \tag{6.}$$

Fig.11(b) plots the measured ventilation rate Q' and predicted values based on $|\overline{\Delta Cp}|$ and $\overline{|\Delta Cp|}$. It can be seen that predicted ventilation rate based on $\overline{|\Delta Cp|}$ generally agrees well with the measured values. The absolute error of the two methods is 104% and 17% respectively.

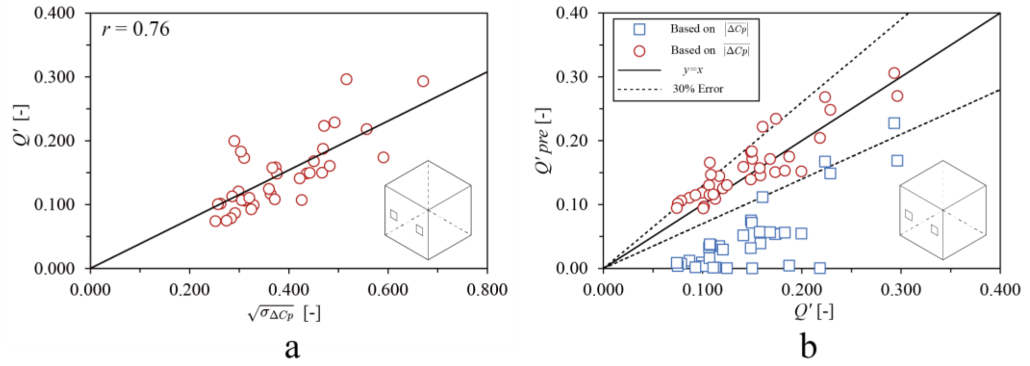

Fig. 11. SS2 ventilation prediction methods (a) Relations between $\sqrt{\sigma_{\Delta Cp}}$ and dimensionless ventilation rate Q'; (b) Comparison between measured Q' and predicted ventilation rate Q'_{pre}

3.6 Relation between SS3 ventilation rate and pressure

To determine the flow rate at each opening for SS3, an initial guess is given to indoor pressure, and the flow rate through 3 openings can be solved independently assuming the flow is purely driven by the difference between indoor pressure and each wind pressure coefficient at the sealed model. The indoor pressure is iterated till the total inflow and outflow rate is conserved. The instantaneous flow rate is half of the total flow rate through 3 openings. Consequently, the ventilation rate of SS3 can be obtained by taking the time average of the instantaneous flow rate. Fig.12(a) shows the flow chart of prediction methods for the ventilation of SS3. This method can also be applied to SS3 or SSn. Fig.12(b) illustrates the predicted and measured ventilation rate. The absolute error of the proposed method is about 17%.

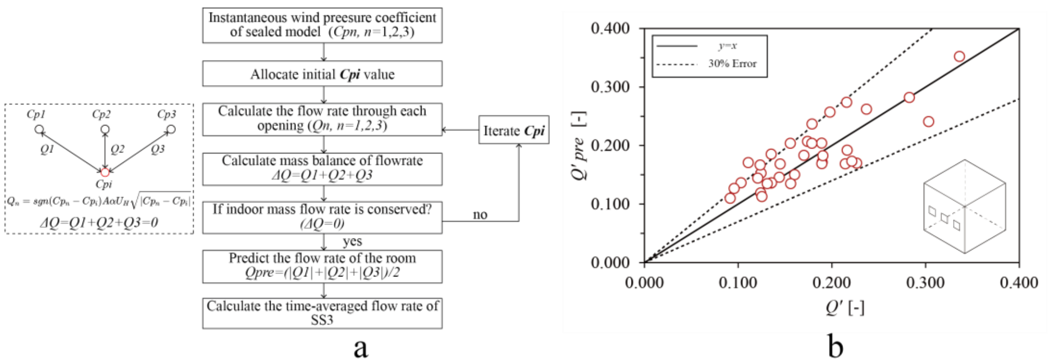

Fig. 12. SS3 ventilation prediction methods (a) The flow chart of prediction methods for ventilation rate of SS3 or SSn; (b) Comparison between measured Q' and predicted ventilation rate Q'_{pre}

4 CONCLUSIONS

The present work reported the wind tunnel experiment to investigate the influence of sheltering buildings as well as discuss simplified ventilation rate prediction methods for wind-induced single-sided ventilation. The following conclusions are summarized as the main understandings of this study:

•In both isolated or sheltered conditions, SS2 has a much higher ventilation rate than SS1, while the ventilation rate of SS3 is only slightly higher than SS2.

•The sheltering does not always reduce ventilation performance of single-sided ventilation. When the wind direction is 120°-180°, higher building density enhances the ventilation performance.

•The ventilation rate of SS1 can be estimated by the wind pressure coefficient, which yields an absolute error of 11% in this study.
•The ventilation rate of SS2 can be predicted using the absolute value of the mean wind pressure coefficient ($|\overline{\Delta Cp}|$), which includes the influence of both steady pressure difference and unsteady pressure fluctuations. The predicted equation only caused a 17% absolute error.
•The ventilation rate of SS3 can be calculated by using the instantaneous wind pressure coefficient from the sealed model and iterating indoor pressure till the inflow and outflow flow rate is conserved, the time-averaged predicted flow rate produced an absolute error of 17%
However, the findings of this work are limited to a reduced-scale model. The similarity of velocity distribution and ventilation rate should be confirmed in the future study, which determines whether the conclusions from this study can be applied to a full-scale scenario.

5 ACKNOWLEDGEMENTS

We would like to thank the AIVC 2023 Reviewers for taking the time and effort necessary to review the manuscript. We sincerely appreciate all valuable comments and suggestions, which helped us to improve the quality of the manuscript.
Part of this work was supported by a JSPS Grant-in-Aid for Scientific Research in Japan (Grant-in-Aid for Scientific Research(B), Grant Number: JP20H02311, Principal Investigator: Tomohiro Kobayashi) and JST SPRING, Grant Number JPMJSP2138.

6 REFERENCES

Adachi, Y., Ikegaya, N., Satonaka, H., & Hagishima, A. (2020). Numerical simulation for cross-ventilation flow of generic block sheltered by urban-like block array. *Building and Environment*, *185*, 107174. https://doi.org/10.1016/j.buildenv.2020.107174

Chu, C.-R., Chiu, Y.-H., Tsai, Y.-T., & Wu, S.-L. (2015). Wind-driven natural ventilation for buildings with two openings on the same external wall. *Energy and Buildings*, *108*, 365–372. https://doi.org/10.1016/j.enbuild.2015.09.041

Daish, N. C., Carrilho da Graça, G., Linden, P. F., & Banks, D. (2016). Impact of aperture separation on wind-driven single-sided natural ventilation. *Building and Environment*, *108*, 122–134. https://doi.org/10.1016/j.buildenv.2016.08.015

Ghiaus, C., Allard, F., Santamouris, M., Georgakis, C., & Nicol, F. (2006). Urban environment influence on natural ventilation potential. *Building and Environment*, *41*(4), 395–406. https://doi.org/10.1016/j.buildenv.2005.02.003

Golubić, D., Meile, W., Brenn, G., & Kozmar, H. (2020). Wind-tunnel analysis of natural ventilation in a generic building in sheltered and unsheltered conditions: Impact of Reynolds number and wind direction. *Journal of Wind Engineering and Industrial Aerodynamics*, *207*, 104388. https://doi.org/10.1016/j.jweia.2020.104388

Ikegaya, N., Hasegawa, S., & Hagishima, A. (2019). Time-resolved particle image velocimetry for cross-ventilation flow of generic block sheltered by urban-like block arrays. *Building and Environment*, *147*, 132–145. https://doi.org/10.1016/j.buildenv.2018.10.015

Jiang, Y., & Chen, Q. (2002). Effect of fluctuating wind direction on cross natural ventilation in buildings from large eddy simulation. *Building and Environment*, *37*(4), 379–386. https://doi.org/10.1016/S0360-1323(01)00036-1

Jiang, Z., Kobayashi, T., Yamanaka, T., Sandberg, M., Kobayashi, N., Choi, N., & Sano, K. (2022). Validity of Orifice equation and impact of building parameters on wind-induced natural ventilation rates with minute mean wind pressure difference. *Building and Environment*, *219*, 109248. https://doi.org/10.1016/j.buildenv.2022.109248

Mohammad, A. F., Ikegaya, N., Hikizu, R., & Zaki, S. A. (2021). Turbulence Effect of Urban-Canopy Flow on Indoor Velocity Fields under Sheltered and Cross-Ventilation Conditions. *Sustainability*, *13*(2), Article 2. https://doi.org/10.3390/su13020586

Shirzadi, M., Tominaga, Y., & Mirzaei, P. A. (2019). Wind tunnel experiments on cross-ventilation flow of a generic sheltered building in urban areas. *Building and Environment*, *158*, 60–72. https://doi.org/10.1016/j.buildenv.2019.04.057

Tominaga, Y., & Blocken, B. (2015). Wind tunnel experiments on cross-ventilation flow of a generic building with contaminant dispersion in unsheltered and sheltered conditions. *Building and Environment*, *92*, 452–461. https://doi.org/10.1016/j.buildenv.2015.05.026